Characterization of new Co and Ru on WC catalysts for Fischer-Tropsch reaction. Influence of the carbide surface state.

Anne Griboval-Constant, Jean-Marc Giraudon, Ivan Twagirashema, Ginette Leclercq, Maria Elena Rivas, Juan Alvarez, Josefina Perez-Zurita, Mireya Goldwasser

▶ **To cite this version:**

HAL is a multi-disciplinary open access archive for the deposit and dissemination of scientific research documents, whether they are published or not. The documents may come from teaching and research institutions in France or abroad, or from public or private research centers.

L'archive ouverte pluridisciplinaire **HAL**, est destinée au dépôt et à la diffusion de documents scientifiques de niveau recherche, publiés ou non, émanant des établissements d'enseignement et de recherche français ou étrangers, des laboratoires publics ou privés.

Characterization of new Co and Ru on α-WC catalysts for Fischer-Tropsch reaction. Influence of the carbide surface state.

A. Griboval-Constant[1] *, J.-M. Giraudon[1], I. Twagishema[1], G. Leclercq[1], and
M.E. Rivas[2], J. Alvarez[2], M. J. Pérez-Zurita[2], M. R. Goldwasser[2].

[1] Unité de Catalyse et Chimie du Solide, UMR CNRS 8181, U.S.T.L., Bâtiment C3, 59655 Villeneuve D'Ascq, Cedex, France.
[2] Centro de Catalisis, Petroleo y Petroquimica, Escuela de Quimica, Facultad de Ciencias, Universidad Central de Venezuela, Apartado 47102, Los Chaguaramos, Caracas, Venezuela.

Key words: CO Hydrogenation, Tungsten Carbide, Cobalt, Ruthenium

* To whom all correspondences should be addressed

E-mail: anne.griboval@univ-lille1.fr

Abstract

An investigation of the performances in Fischer-Tropsch reaction of 1wt% M/WC(X) (M = Co, Ru; X = A, B), where A is a tungsten carbide protected by free carbon and B is a clean tungsten carbide, was carried out. Supported catalysts performances were compared to those of the parent tungsten carbides at 473 K and 20 bar. It was found that WC(A) produces mainly hydrocarbons but also 20-40% alcohols, whereas WC(B) activity is only towards linear alkanes. Before catalytic test, a reduction in pure hydrogen allows obtaining Co^0 and Ru^0 dispersed on layers of free carbon covering the WC core for the WC(A), and on a surface free of oxygen for WC(B). Co as Ru dispersions are improved on WC(B) compared to WC(A). A direct consequence is that Co/WC(B) has a better activity than Co/WC(A). Ru-W alloy formation could be responsible of the inobservance of a better activity for Ru/WC(B). On contrary, addition of Ru on WC(A) highly increases the activity and the production of heavy hydrocarbons. This beneficial effect, not observed with cobalt, could be attributed to a better dispersion of ruthenium on a carbon polymeric surface of WC.

1. Introduction

The world stocks of natural gas increase continuously and represent at present the estimates of the world wild resources crude oil. Valorization of this natural gas induces a renewed interest for the Fischer-Tropsch reaction which is one of the major routes of natural gas utilization.

The Fischer-Tropsch reaction can lead to a broad range of products, i.e. hydrocarbons, alcohols, acids, esters, … from a mixture of carbon monoxide and hydrogen. FT synthesis proceeds on supported transition metal catalysts, Co or Fe on oxide supports generally Al_2O_3 or SiO_2 [1-3]. By opposition few works have been carried out on carbon related supports [4-6]. Conventional FT catalysts are prepared via aqueous impregnation of porous oxide supports with solutions of various metal salts. Among the different parameters affecting the catalytic performances, the nature of the support is a key factor. The major drawback of silica and alumina supports is the formation of cobalt aluminate or silicate during the calcination of cobalt precursor. Cobalt incorporated in these phases is not reduced during hydrogen treatment before catalytic test at conventional temperature. Hence the amount of available metallic cobalt for FT reaction is significantly reduced, leading to a decrease of the activity. Similarly selectivity can be tuned by the nature of the support. For example, ruthenium which is a well-known metal to have the capacity to increase the alkane chain length produces heavy alcohols when dispersed on a reducible support (MoO_3, WO_3) [7]. Such a behavior can be account by a reaction scheme, which includes cooperation between the metallic sites and the oxygen vacancies on the support at the edge of the metallic particles [8].

Among the group VI transition metal carbides, the hexagonal tungsten carbide WC is a remarkable material in the sense that it combines physical and catalytic properties suitable for FT reaction. Indeed it has good mechanical properties, a high density (2.54 g.cm^{-3} for WC compared with 0.84 g.cm^{-3} for Al_2O_3) and a high thermal conductivity λ (expressed at 20°C in

W.m^{-1}.K^{-1}: 26-35 for Al$_2$O$_3$, 60-80 for WC and 63-155 for SiC) [9]. Such properties are relevant to Fischer-Tropsch reaction conditions, which is a highly exothermic process that operates at moderate pressure. I. Kojima et al. have previously shown that group VI transition metal carbides (particularly molybdenum and tungsten based catalysts) are active for FT reaction [10]. L. Leclercq [11] and H.C. Woo [12] have reported that tungsten and molybdenum carbides produced mainly light alkanes, whereas the formation of alcohols is related to the surface stoichiometry and to the extent of carburization [11].

Both the use of cobalt or ruthenium as active metals for FT reaction and the physical and catalytic performances of group VI transition metal carbide have motivated a fundamental study of the influence of the nature of transition metal carbides (M'$_x$C with M'= W, Mo; x = 1 or 2) on the cobalt or ruthenium reactivity. In a recent study we have reported the catalytic performances of 1%wt Co or Ru dispersed on Mo$_2$C [13]. It was found that Mo$_2$C gives mainly light hydrocarbons, alcohols and CO$_2$. As Mo$_2$C intrinsic nature is to form light hydrocarbons, carbon vacancies or/and remaining oxygen adsorbed on the surface can account into alcohol formation. Addition of Ru or Co increases the activity following the sequence: Mo$_2$C < Ru/Mo$_2$C < Co/Mo$_2$C. The addition of ruthenium decreases alcohol formation whereas cobalt increases formation of heavy hydrocarbons.

The aim of this work is to study the performances of 1wt% M/WC(X) (M = Co, Ru; X = A, B) where A is a tungsten carbide protected by free carbon and B is a clean tungsten carbide. WC(A) and WC(B) were synthesized in order to discriminate the physical and catalytic properties of the tungsten carbide on catalytic performances of the solids. Indeed layers of carbon passivate the tungsten carbide surface of WC(A) while free carbon has been removed from WC(B). It is expected that the performances of M/WC(A) benefit only to the physical (mechanical resistance, high density and thermal conductivity) properties of inactive

tungsten carbide due to the deposit of free carbon layers at the surface. On the contrary, the reactivity of supported metal can depend both on physical and catalytic properties of WC(B).

The catalysts have been extensively characterized by elemental analysis, nitrogen adsorption, X-ray diffraction (XRD), H_2-TPR, X-ray photoelectron spectroscopy (XPS). The characterizations are discussed together with the catalytic performances of the samples in Fischer-Tropsch synthesis.

2. Experimental

2.1. Preparation of the catalysts

2.1.1. Synthesis of tungsten carbide

Bulk tungsten carbides were prepared by a Temperature Programmed Experiment.

A precursor oxide WO_3 (10 g) (Fluka, 99.9% purity) was first heated at 823K for 10 h in flowing nitrogen (10 $l.h^{-1}$) and reduced and carburized in a mixture of 20% CH_4-H_2 at a flow rate of 10 $l.h^{-1}$ from room temperature to a final value of 1073 K (β = 60 $K.h^{-1}$). The isotherm was maintained for about 8 h. After cooling down to room temperature, the mixture of methane-hydrogen was replaced by a N_2 flow (10 $l.h^{-1}$) for one hour. By this procedure a tungsten carbide protected by free carbon on the surface was obtained [14].

The experimental procedure described above was completed by a cleaning step in order to remove free carbon from the tungsten carbide surface. After carburization, the sample was submitted to a flow of pure H_2 (8 $l.h^{-1}$) from ambient temperature to 1073 K (100 $K.h^{-1}$). The final temperature was kept for one hour. Carbon removal was followed on line by the detection of methane with gas chromatography analysis. The sample was then submitted to a flow of N_2 (10 $l.h^{-1}$) for one hour before to be passivated at room temperature in a 2 % O_2-N_2 mixture for 2h (3 $l.h^{-1}$) to protect the catalyst against deep oxidation.

Hereafter the solids will be noted WC(A) for tungsten carbide protected by free carbon and WC(B) for clean tungsten carbide.

2.1.2. Synthesis of supported catalysts

The catalysts were obtained by wet impregnation of tungsten carbide with an aqueous solution of respectively ruthenium chloride dihydrate (Fluka, purum, ≈ 38-40% Ru) or cobaltous nitrate hexahydrate (Fluka, ≥ 98 % purity), in order to have a nominal content of 1wt% Ru or Co. After slow evaporation of the solvent, the solids were dried at 393K overnight. Hereafter the solids will be denoted M/WC(A) and M/WC(B), where M is the Co or Ru metal.

2.2. Physical characterizations

Elemental analysis. The chemical analyses of the supported catalysts were determined by atomic absorption for Co, W and Ru and by coulometry for C, by the Central Service of Chemical Analysis of the CNRS (Vernaison, France).

Surface area. The B.E.T. surface areas were measured by a single point BET method using a QUANTASORB J.R. apparatus. Before experiment, the fresh catalysts were outgassed in a flow of nitrogen for 30 mn at 423K.

X-ray diffraction. XRD patterns were recorded at room temperature by a SIEMENS D5000 diffractometer using Cu K_α radiation.

XPS. The X-ray photoelectron spectra (XPS) were recorded with a VG ESCALAB 220XL spectrometer equipped with a monochromatized Al source (Al K_α = 1486.6 eV). The analyser was operating in a constant pass energy mode (E_{pas} = 30 eV) using the electromagnetic mode for the lens. The resolution measured on Ag $3d_{5/2}$ peak was 0.75 eV. Due to the metallic and conducting character of the samples, no charge effect was observed

and its neutralization was not required. The calibration of the samples in binding energy was based on three photopeaks: Cu $2p_{3/2}$ (928.7 eV), Ag $3d_{5/2}$ (368.3 eV) and Au 4f (84 eV). Spectrums of all solids were recorded before and after reduction in flowing hydrogen. The reduction of the catalysts was carried out in a flow of pure hydrogen (2 $l.h^{-1}$) in the preparation chamber close to the analysis chamber for 5 h at 673 K for Ru and 673 or 773 K for Co based catalysts (β = 3 $K.min^{-1}$). For ruthenium catalysts, simulations of XPS spectrums of (C 1s + Ru 3d) level peaks are performed by the Eclipse Software (Thermo VG Scientific).

H_2-TPR. Temperature program reduction experiments were performed by passing 5% H_2/Ar gas mixture through the catalyst while increasing temperature at a linear rate. The amount of samples was about 200 mg. The gas flow velocity was 50 $ml.mn^{-1}$; the rate of temperature ramping was 5 $K.min^{-1}$. The reduction gas mixture was purified with the use of water and oxygen traps. The gaseous products evolved at the outlet of the reactor were analyzed by mass-spectroscopy (OMNISTAR).

2.3. Catalytic activity measurement

The catalytic tests were performed in a stainless steel fixed-bed flow reactor operating at 473-533 K and total pressure of 20 or 50 bar with VSV equal to 6000 h^{-1} (VSV : Volumetric Space Velocity defined as the reactant gas flow divided by the catalyst volume). Hydrogen (99.995 %, Air liquide) and carbon monoxide (99.94 %, Air liquide) were supplied to the reactor through mass flow controllers (Brooks). The H_2/CO ratio was 2 in all experiments. N_2 (0.3 $l.h^{-1}$) was used as internal standard. The catalyst loadings were of about 2.5-2.7 g.

Prior to the catalytic test, all the samples were activated in a flow of pure hydrogen (3.6 $l.h^{-1}$, 12h) at atmospheric pressure from room temperature either to 673K for WC(A), WC(B) and Ru based catalysts, and 773K for Co based catalysts. The temperature of

reduction was chosen in order to get Co or Ru at the metallic state. The catalysts were then cooled to the initial reaction temperature (473 K), and the pressure was increased in a H_2-N_2 flow up to 20 bar. Then the H_2 and N_2 flows were adjusted to the values of the reaction test and CO was introduced. To avoid a possible condensation of the reaction products, gas transfer lines were continuously heated at 393 K. Analysis of the gaseous products were carried out on line with a gas chromatograph (Varian 3400) equipped with TCD and FID detectors with CTR-1 for C1 products and a Tenax column for hydrocarbons (C_1-C_{10}) and alcohols up to C_3, respectively. High-molecular-weight products (C_{10}^{+} hydrocarbons) were collected from a hot condenser heated at 393K. The wax analysis was performed on a WCOT ULTI-METAL column (coating HT SIMDIST CB). Catalytic rates and selectivities were measured at the stationary regime after circa 24 h time-on-stream. The conversion X, expressed in percentage, is the ratio of the number of moles of CO converted to the initial number of moles of CO. Specific reaction rates, expressed in $mol.h^{-1}.g^{-1}$, were defined as the number of moles of CO converted per unit time per gram of catalyst. Product selectivity (S) was reported as the percentage of CO converted into a given product expressed in C atoms, excluding CO_2. $S(C_n)$ and $S(C_{5+})$ were referred respectively to the selectivity in hydrocarbons with n carbon atoms and to the selectivities of all hydrocarbons in the gas phase with a carbon atom number higher than or equal to 5. By the same way, S(COH) is the global selectivity in alcohols. Carbon mass balances were respected within the margin of error of around 20 % for all catalysts.

3. Results

3.1. Catalyst characterizations

3.1.1. Fresh catalysts

3.1.1.1. Tungsten carbide

Figure 1 shows the variation of the area of CH_4 obtained by CPG during the cleaning procedure in order to obtain WC(B). The sample is submitted to a flow of pure H_2 (8 l.h^{-1}) while temperature increased from ambient temperature to 1073 K (β = 60 K.h^{-1}). This temperature is maintained for one hour. The concentration of methane starts at 847 K, increases, exhibits a maximum at 909 K and then decreases to show a shoulder before to reach a constant value. As soon as the methane pressure was residual, the temperature was allowed to decrease slowly from 1073 K to room temperature in pure H_2. The peak production corresponds to the removal of free carbon while the shoulder is related to the removal of the first carbidic carbon layer. At 1073 K the CH_4 partial pressure (7.10^{-4} atm) is slightly lower than that at equilibrium: $WC_{surface} + (2x) H_2 \leftrightarrow WC_{1-x, surface} + x CH_4$ in accordance with the fast replenishment of the surface by carbon diffusion from the bulk [15]. Hence a tungsten carbide with a homogeneous composition is here expected.

The X-ray diffraction pattern of WC(A) is characteristic of a simple hexagonal structure of WC (Fig. 2d). For WC(B) the lines at 2Θ = 40.2 and 58.5 characterize W metal which amounts for about 15 % (cf Annexe) along the WC phase (Fig. 2a). Chemical analysis give a global atomic C/W ratio of 1.4 for WC(A) in accordance with an excess of carbon deposited on WC (Table 1). For WC(B) sample, rid of free carbon, the C/W ratio of 0.7 clearly shows that free carbon as a significant fraction of carbidic carbon have been removed as stated above.

Surface characterization has been performed by XPS (Table 2). The W 4f signal of WC(A) and WC(B) samples shows a doublet at binding energies of 31.7 eV (W $4f_{7/2}$) and 33.7 eV (W $4f_{5/2}$) characteristic of tungsten carbide (Fig. 3) [16-17]. The W $4f_{7/2}$, W $4f_{5/2}$ components at around 35 and 37 eV indicate the presence of some (W^{+6}) surface oxide species. This oxide fraction amounts to 0.10 and 0.26 of the total W 4f signal respectively for WC(A) and WC(B) (Table 3). Such discrepancies are in accordance with a tungsten carbide

surface covered with free carbon or not. Indeed, after air exposure, the WC(A) carbide surface is protected from the excess carbon whereas a W^{6+} phase is induced during the passivation step for WC(B).

For the two samples, the C 1s spectrums show two peaks which evidence carbidic carbon (B.E. = 282.8 eV [18]), free carbon (B.E. = 284.5 eV) and a tail at higher binding energy values (B.E. at about 288 eV) relative to oxidized carbon (Fig. 4). The free carbon arising in the C 1s peak at 284.5 eV for WC(B) results from a contamination in the spectrophotometer, whereas for WC(A), it is mainly due to carbon deposit arising from CH_4 decomposition. The C/W ratio determined by XPS analysis (Table 3) is substantially higher than that measured by chemical analysis for WC(B) (Table 1). This shows that most of the carbon is localized at the surface of the carbide. The XPS C_c/W_c (carbidic carbon to tungsten in the reduced phase) atomic ratio values of 1.10 and 0.82 for WC(A) and WC(B) are in accordance with a stoechiometric WC surface taking into account the margin of error which is about 20 %. It is worth mentioned that the small binding energy difference between tungsten carbide and metal tungsten of circa 0.5 eV precludes here to evidence the metal tungsten phase.

The total surface area of the catalysts was low (< 10 $m^2.g^{-1}$) (Table 1), but the aim of the preparation was to obtain tungsten carbides with well-defined structure and not to optimize the specific surface of the material.

3.1.1.2. Supported catalysts

The X-ray diffraction patterns of the WC supported Co and Ru catalysts are rather similar with that of the tungsten carbide parent (Fig. 2). It is worthy to mention that the proportion of the metallic tungsten phase decreases by impregnation of WC(B) with aqueous solution of cobalt or ruthenium. Tungsten metal likely reoxidized during the impregnation to

give an amorphous oxide phase not detected by XRD. Due to the low metal content, no metal (Co or Ru) phases were detected. Co and Ru weight percentage of the samples (Table 1) was closed to the expected 1wt% value. The specific surface areas were in accordance with the parent sample ones.

The Ru 3d, Co 2p, W 4f, C 1s XPS spectrums of the supported catalysts are reported figues 5 to 8.

For the WC supported ruthenium catalysts, the Ru 3d signal extracted from the C 1s envelope (Table 2, Fig. 5a and 5b) exhibits a Ru $3d_{5/2}$ peak at B.E. around 281.7-281.9 eV characteristic of Ru^{3+} [19]. WC supported cobalt catalysts exhibit the Co $2p_{1/2}$ and Co $2p_{3/2}$ binding energies respectively at around 796.4-797.2 eV and 780.9-781.2 eV. Those values and the intense shake-up satellite structures are in agreement with the presence of Co^{2+} ions at the surface (Table 2, Fig. 6a and 6d) [20, 21]. It is worth mentioning that the M/W_T XPS atomic ratio substantially increases (0.13 to 0.49 for Ru, 0.15 to 0.96 for Co) changing from A to B support (Table 3).

The C 1s and W 4f envelops and the atomic ratios W_c/W_T and C_C/C_T for WC supported ruthenium and cobalt catalysts compared with WC(A) keep unchanged (Table 3), showing that WC(A) is inert towards aqueous solution during impregnation.

The XPS W_c/W_T atomic ratios of Ru or Co on WC(B) of 0.46 are substantially less than that of WC(B) of 0.74 in accordance with an increase of the well characterized W $4f_{5/2}$-W $4f_{7/2}$ doublet of W^{6+} (Fig. 7a and 7b, Table 3). This increase of the oxide W^{6+} phase as the decrease of the W metal phase in the bulk of the samples clearly show that the tungsten carbide surface corrodes in aqueous solution during impregnation.

3.1.2. Catalysts activated by hydrogen

Before catalytic test, a reduction of the catalysts by hydrogen is necessary to obtain cobalt and ruthenium at the metallic state considered as the active species for Fischer-Tropsch reaction. H_2-TPR experiments and XPS analysis have been carried out in order to get a better comprehension of this H_2 pre-treatment.

a) H_2-TPR experiments

The H_2-TPR profiles of the WC(B) based catalysts are given on Figure 9. For Co/WC(B) and Ru/WC(B) samples the gaseous products evolved from the exit of the reactor have been monitored by mass-spectroscopy.

For WC(B), the H_2-TPR profile of WC(B) shows a very small consumption of hydrogen from about 650 to 900 K (Fig. 9a). This slight consumption is likely due to the removal of oxygen atoms from the passivation layer as water [22].

The H_2 trace of Co/WC(B) has a complex envelop which consists of a small peak at 491 K and two high peaks at 677 K and 855 K (Fig. 9b). By mass-spectroscopy, we first observe around 420 K an increase of m/e = 16, 17, 28, 44 signals having a maximum at 491 K, before to decrease to about 550 K (Fig. 10a). As the temperature is raised, additionally m/e = 16, 28 and 44 signals are observed: between 575 and 750 K (m/e = 16 and 44), between 625 and 800 K (m/e = 28). The m/e = 17 is associated with the removal of NH_3, arising from the reduction of the nitrate anions relative to the cobaltous precursor. The associated m/e = 16 signal having the same profile as m/e = 17 readily excludes CH_4 production. The simultaneous m/e = 28 and 44 signals are respectively assigned to the CO and CO_2 productions, due to oxygen removal from the passivation layer. As the temperature is raised, the m/e = 16, 44 signals, which are detected between 575 and 800 K, are ascribed to CH_4 and CO_2, related to the removal of some adventitious carbon. The assignation of the last broad signal m/e = 28 is difficult as it could be assigned to N_2 and/or to CO production respectively

related to the reduction of the remaining nitrate moieties and/or to the removal of strongly adsorbed oxygen.

The H_2-trace of the Ru/WC(B) catalyst is only composed of two peaks: a large one centred at 417 K and another small one at 539 K with a long tail toward high temperatures (Fig. 9c). The first H_2 consumption step is associated with a very weak CO_2 production, while removal of CO (490 - 600 K) and CH_4 occur (480 - 800 K) in the second step (Fig. 10b). Such signals are again assigned to the removal of oxygen and carbon weakly bound to the surface of the catalyst.

H/Ru atomic ratio of 3.7 for the first peak of H_2 consumption (300-480 K) is higher than the expected value of 3.0 corresponding to the complete reduction of Ru^{3+} into Ru metal (Table 4). This difference is likely due to the removal of oxygen mainly incorporated during the passivation step as H_2O which is not seen here because it is trapped before TCD detection. The second peak is the removal of oxygen and carbon impurities weakly bound to carbidic surface.

For Co/WC(B) the first H_2-TPR peak is related to the thermal reduction of nitrate species into ammonia. However, partial reduction of Co^{2+} can not be ruled out in spite of the low temperature. In the second step (peak at 677 K), reduction of cobalteous species into metallic cobalt occurs, then removal of oxygen and carbon entities weakly bound to the surface happen.

To conclude H_2-TPR experiments carried out on WC(B) species have clearly shown that the Ru^{3+} cation as expected is more easily reduced than Co^{2+} and that most of the impurities originating mainly from the passivation step are removed to give Co and Ru metal on a clean tungsten carbide surface.

b) XPS experiments

The reduction temperature before catalytic testing has been chosen at 673K for Ru and 773K for Co based catalysts in order to ensure to get the metal species totally reduced. XPS measurements have been carried out after submitting the four different samples to a flow of hydrogen from room temperature to a final temperature kept for 5 hours: 673K for Ru and Co based catalysts and 773K for Co/WC(A) (see experimental section).

After H_2 pre-treatment, the Ru $3d_{5/2}$ peak initially observed at 281.7-281.9 eV characteristic of Ru^{3+} shifts to lower B.E. values (279.8-280.2 eV) which agrees with a Ru^0 non interacting with the support [23-25] (Table 2, Fig. 11a-b). After reduction at 673 K the Co 2p spectrums (Fig. 6b and 6e) show a well resolved Co $2p_{1/2}$-Co $2p_{3/2}$ doublet at 793.2-778.4 eV characteristic of the Co^0 phase [21, 26-27]. Along the Co $2p_{3/2}$ peak at 778.4 eV is a small signal at 780.9 eV corresponding to a fraction of non reduced Co^{2+} which totally disappears after reduction at 773 K (Fig. 6c).

For WC(B) supported Co and Ru catalysts, the C 1s signals only show a peak at 282.7 eV corresponding to carbidic carbon (Fig. 8e and 11b, Table 3). The initial component at 284.6 eV of adventitious carbon is almost totally removed. Moreover, W 4f spectrums (Fig. 7c-d) show that of the W $4f_{5/2}$ - W $4f_{7/2}$ doublet at 37.2-35.2 eV characteristic of W^{+6} species almost disappeared. All these observations are in agreement with the removal of impurities from the carbide surface. The WC(A) based catalysts have XPS composition, which keep practically unchanged before and after reduction, showing that the only effect of the H_2 treatment is to reduce Ru and Co cations into metallic state (Table 2 and 3).

The evolution of the XPS Ru/W_T and Co/W_T atomic ratios before and after reduction, which is related to the dispersion of the metal, has been investigated (Table 3). On WC(A) based catalysts, the similar Ru/W_T (0.13) and Co/W_T (0.15) initial ratios seem to indicate a

better dispersion of ruthenium, taking into account that the atomic weight of Ru is about two times higher than the Co one. The decrease of the Co/W_T ratio from 0.15 to 0.10 (673 K) and 0.08 (773 K) after reduction can be explained by an onset of coalescence of the cobalt metallic particles, contrarily to the Ru/WC(A) catalyst whose Ru/W_T ratio keeps unchanged after reduction at 673 K. The Co/W_T value of 0.96 twice as the Ru/W_T one of 0.49 is indicative of a rather similar dispersion for the Co and Ru on WC(B). After reduction at 673 K, the Ru/W_T and Co/W_T ratios substantially decrease strongly suggesting an increase of the metallic particle size, higher for Co than for Ru. Moreover the dispersion of Co and Ru is always lower over WC(A) than WC(B).

To sum up, XPS results clearly show that the H_2 pre-treatment leads to Co and Ru metallic particles dispersed on a carbon layer covering tungsten carbide and on tungsten carbide respectively for M/WC(A) and M/WC(B) catalysts.

3.2. Catalytic behaviour

3.2.1. Tungsten carbide

For WC(A), catalytic test has been carried out in steps which allow to vary one parameter, i.e. temperature or pressure. Conversion and selectivities reported in table 5 have been obtained at steady state, when the relative variation of conversion is less than 5% and the carbon selectivities unchanged within the margin of error that is for duration of 24 h. At 20 bar variation of the temperature from 473K to 533 K increases five times the CO hydrogenation activity. Hence WC(A) is active for the FT reaction but the conversion remains low. Product distribution at 473K and 20 bar (Table 5) is as follow: mainly light alkanes (C_1-C_4: 63%), higher alkanes up to C_{10} (C_{5+}: 15%) and alcohols (COH: 22%). As temperature is increased, formation of light alkanes increases at the expense of C_{5+} and alcohol production. A similar behaviour is obtained at 50 bar. All these observations are consistent with previous

works which have shown that the production of light products is favoured by an increase of the reaction temperature [28]. Noteworthy CO_2 production is only observed for the highest temperature here of 533 K.

For comparison, WC(B) has been studied by catalytic test realized at 473K and 20 bar (Table 6). The conversion is low as for WC(A). WC(B) gives light alkanes (C_1-C_4: 78%) and heavier alkanes (C_{5+}: 22%), with no alcohol production.

3.2.2. Study of WC supported Ru and Co catalysts

WC supported Ru and Co catalysts have been tested at 473 K for a pressure of 20 or 50 bar. Their catalytic performances have been compared to those of the parent tungsten carbides (Table 6).

At 473K and 20 bar, addition of Co on WC(B) increases markedly the conversion whereas no such effect is observed with WC(A). Co/WC(A) gives light alkanes (C_1-C_4: 48%), higher alkanes up to C_{10} (C_{5+}: 46%) and alcohols (COH: 6%), while Co/WC(B) produces only alkanes (C_1-C_4: 59%, C_{5+}: 41%). Addition of cobalt on tungsten carbides increases the length of the alkane chain and when dispersed on WC(A) decreases alcohol production. For Co/WC(A) a raise of the pressure from 20 to 50 bar induces an increase of the conversion up to 4 % and favours both C_{5+} and alcohol productions.

Contrarily to cobalt, at 473 K and 20 bar, while the conversion of Ru/WC(B) is rather similar to that of WC(B), it is higher on Ru/WC(A). Gaseous phase selectivity relative to the two samples also markedly differs. Thus the selectivity to alkanes (C_1-C_4: 72%, C_{5+}: 28%) of Ru/WC(B), which resembles that of WC(B), is totally changed for Ru/WC(A) (C_1-C_4: 13%, C_{5+}: 87%). Here high hydrocarbons are also trapped in the hot condenser (heated at 393 K) at 473 K whatever the pressure (for 24 h : 0.67 g at 20 bar, 2.39 g at 50 bar). The hydrocarbons cuts at 20 and 50 bar are: C_{10}-C_{50} and C_{10}-C_{45} and are centered at about 20 carbon atoms (Fig.

12). The values of α which is the probability of chain growth [29], calculated from the C_{20}-C_{40} cut, of about 0.8 are little influenced by the total pressure.

4. Discussion

After synthesis the two tungsten carbides differ from their surface state which consists respectively in polymeric carbon and oxide species for WC(A) and WC(B). Based from XPS results, ruthenium is better dispersed than cobalt on the polymeric carbon layer. As Ru dispersion is maintained after reduction in hydrogen, cobalt particles begin to coalesce. By contrast, cobalt and ruthenium species dispersed on oxide layer are much prone to aggregation after hydrogen pre-treatment.

Conversion of WC(A) and WC(B) are similar in the FT reaction despite free carbon removal after carburization by a H_2 treatment for WC(B) on contrary to WC(A). The activity on WC(A) could be explained by the occurrence of a porous carbon layer, which allows the diffusion of H_2 and CO reactants to the active sites of the carbide. The striking difference in selectivity between WC(A) and WC(B) is that alcohol production occurs on WC(A). Methanol and to a less extent ethanol and propanol are formed on WC(A). It is likely that the presence of the tungsten metal, which is well-known to dissociate CO, is able to hydrogenolyse the alcohols. Nevertheless selectivity of the two catalysts is mainly towards hydrocarbons in agreement with the literature [11]. They favour light hydrocarbons production compared to C_{5+} formation.

Based on the M/W_T XPS atomic ratios a better activity is expected on the WC(B) supported Ru and Co catalysts. If it is confirmed in the case of Co, on the other hand Ru/WC(B) is poorly active. A tentative explanation of the low activity of the Ru/WC(B) catalyst could be related to the formation of a Ru-W solid solution. In fact, close values in the metallic atomic radius of ruthenium (1.35 Å) and tungsten atoms (1.37 Å) allows solid-

solution formation. Indeed, the solubility of W atoms in Ru is very high even at low temperatures, so it is energetically favorable for W atoms to diffuse into the Ru overlayers and form stable phases or alloys [30]. A previous studies related to the deposition of ruthenium overlayers on tungsten single crystals has clearly shown that incremental dosing of Ru causes intermixing of the ruthenium and tungsten atoms at the interface, even at fractional monolayer coverages [30]. Nevertheless, a specific interaction (electronic or geometric) between the ruthenium particles and the tungsten carbide can also affect the catalytic properties of the sample. Besides, the marked activity discrepancies between Co/WC(B) and Ru/WC(B) seems to be hardly explain based on the second hypothesis, suggesting alloy formation. At present it is not possible to formally discriminate one hypothesis in comparison with the other.

Introduction of cobalt on tungsten carbide WC(A) has not significant effect on activity contrarily to ruthenium, Ru/WC(A) is the most active catalyst. Such a higher activity can be explained by a better ruthenium dispersion on WC(A) as reflected by a higher Ru/W_T XPS ratio. The polymeric carbon layer covering the tungsten carbide here favors the ruthenium dispersion compared to the cobalt one. Ru/WC(A), and Co/WC(A) to a less extent, produce more higher alkanes (at 20 bar 473 K, C_{5+}: 87% Ru/WC(A); 46% Co/WC(A)) than the parent tungsten carbide (15.3%). The C_{5+} production increase is in accordance with the presence of Co or Ru, which are well-known to favour the chain length of hydrocarbons. Alcohol production decreases by four-fold after impregnation of Co, able to hydrogenolyze such oxygenate compounds. The non detection of alcohol on Ru/WC(A) can be explained in a similar manner.

Addition of Co to WC(B) increases the activity of the catalyst contrarily to WC(A) in agreement with a better cobalt dispersion. An enhancement of the C_{5+} hydrocarbons production correlates with a higher number of cobalt metallic active sites. By opposition, as

stated above, ruthenium addition on WC(B) has practically no effect on activity and selectivity. As stated above, the formation of a Ru-W alloy or specific interaction between ruthenium particles and tungsten carbide could tame here the metal Ru catalytic behavior.

5. Conclusion

An investigation of 1% Co and Ru dispersed on bulk α-WC covered either with polymeric carbon layers (WC(A)) or oxygen species (WC(B)) was carried out in the CO/H_2 reaction and compared with the parent tungsten carbide. It was found that WC(B) gives only linear alkanes while WC(A) produces 20-40 % alcohols together with hydrocarbons. After H_2 pre-treatment cobalt and ruthenium species are totally reduced to give M^0/WC and M^0/C/WC (M = Co or Ru) as polymeric carbon has not been removed from WC(A). Co and Ru dispersions are improved on WC(B) compared to WC(A). A direct consequence is that Co/WC(B) has a better activity than Co/WC(A). Ru-W alloy formation could be responsible of the inobservance of a better activity for Ru/WC(B). On the other hand, a better dispersion of Ru compared to Co on WC(A) is responsible for a higher activity and a great enhancement of the chain growth of hydrocarbons.

Acknowledgements

Annexe

Atomic metal tungsten percentage has been evaluated by the formula:

$$\% \ W \ metal = \frac{\dfrac{I_W}{I_{Wref}}}{\dfrac{I_W}{I_{Wref}} + \dfrac{I_{WC}}{I_{WCref}}}$$

I_W: intensity of the $2\Theta = 40.2\ °$ line in the sample

I_{Wref}: intensity of the $2\Theta = 40.2\ °$ line in the pure W compound

I_{WC}: intensity of the $2\Theta = 48.3\ °$ line in the sample

I_{WCref}: intensity of the $2\Theta = 48.3\ °$ line in the pure WC compound

References

[1] M.E. Dry, Catalysis Today 71(2002) 227.

[2] E. Iglesia, S.C. Reyes, R.J. Madon, and S.L. Soled, Adv. Catal. 39 (1993) 221.

[3] E. Iglesia, Appl. Catal. A : General 161 (1997) 59.

[4] A. Guerrero Ruiz, J.D. Lopez Gonzalez, I. Rodriguez Ramos, J. Chem. Soc., Chem. Commun. (1984) 1681.

[5] W.-P. Ma, Y.-J. Ding, L.-W. Lin, Ind. Eng. Chem. Res. 43 (2004) 2391.

[6] J. Xiong, Y. Ding, T. Wang, L. Yan, W. Chen, H. Zhu, Y. Lu, Catt. Lett. 102(3-4) (2005) 265.

[7] M.J. Pérez-Zurita, M. Dufour, Y. Halluin, A. Griboval, L. Leclercq, G. Leclercq, M.R. Goldwasser, M.L. Cubeiro, G. Bond, Appl. Catal. A: General, 274 (2004) 295.

[8] Y. Halluin, P.D.H. Thesis, "Catalyseurs à base de ruthénium modifié pour la synthèse d'alcools lourds à partir du gaz de synthèse", Lille (1998).

[9] Handbook of chemistry and physics, 85th edition, 2004-2005.

[10] I. Kojima, E. Miyazaki, I. Yasumori, J.C.S. Chem. Comm. (1980) 573.

[11] L. Leclercq, A. Almazouari, M. Dufour, G. Leclercq, in "the Chemistry of Transition Metal Carbides and Nitrides" (S.T. Oyama, Ed.), Blackie, Glagow, (1996) 345.

[12] H.C. Woo, K.Y. Park, Y.G. Kim, I.S. Nam, J.S. Chung, and J.S. Lee, Appl. Catal. 75 (1991) 267.

[13] A. Griboval-Constant, J.-M. Giraudon, G. Leclercq, L. Leclercq, Appl. Catal. A 260 (2004) 35.

[14] G. Leclercq, M. Kamal, J.M. Giraudon, P. Devassine, L. Feigenbaum, L. Leclercq, A. Frennet, J.M. Bastin, A. Löfberg, S. Decker, M. Dufour, J. Catal. 158 (1996) 142.

[15] L. Delannoy, J.-M. Giraudon, P. Granger, L. Leclercq, G. Leclercq, J. Catal. 206 (2002) 358.

[16] L. Leclercq, M. Provost, et al., J. Catal. 117 (1989) 371.

[17] J. Lemaître, B. Vidick, B. Delmon, J. Catal. 99 (1986) 415.

[18] T.P.St Clair, S.T. Oyama, D.F. Cox, S. Otani, Y. Ishizama, R-L Lo, K-I. Fukui, Y. Iwasawa, Surface Science 426 (1999) 187.

[19] C. Malitesta, G. Morea, L. Sabratin, P.G. Zambonin, Annali di Chimica (1998) 473.

[20] J.P. Bonnelle, J. Grimblot, A. D'Huysser, J. Electron spectr. 7 (1975) 151.

[21] R. Bechara, D. Balloy, D. Vanhove, Appl. Catal. 207 (2001) 343.

[22] A. Frennet, G. Leclercq, L. Leclercq, G. Maire, R. Ducros, M. Jardinier-Offergeld, F. Bouillon, J-M Bastin, A. Löfberg, P. Blehen, M. Dufour, M. Kamal, L. Fiegenbaum, J.-M. Giraudon, V. Keller, P. Wehrer, M. Cheval, F. Garin, P. Kons, P. Delcambe, L. Binst, Proceeding of the 10th international Congress on Catalysis (1992) 144.

[23] C. Malitesta, G. Morea, L. Sabratin, P.G. Zambonin, Annali di Chimica (1998) 473.

[24] K.S. Kim, N. Winograd, J. Catal. 35 (1974) 66.

[25] Y.C. Chen, S.C. Huang, W.J. Wang, J. Chin. Inst. Chem. Eng. 19(5) (1988) 263.

[26] L.A. Bruce, M. Hoang, A.E. Hughes, T.W. Turney, Appl. Catal. *A*. 100 (1993) 51.

[27] Z. Zoldos, L. Guczi, J. Phys. Chem. 96 (1992) 9393.

[28] P. Chaumette, Rev. Inst. Fr. Pétrole 51 (1996) 711.

[29] P.J. Flory, J. Am. Chem. Soc. 58 (1936) 1877.

[30] M.J. Gladys, G. Jackson, J.E. Rowe, T.E. Madey, Surface Science 544 (2003) 193.

22

Table 1

Characterization of the catalysts

catalyst	Me (wt%)	C (wt%)	W (wt%)	Atomic ratio C/W	S_{BET} $(m^2.g^{-1})$
WC(A)	-	8.36	91.63	1.4	6
Ru/WC(A)	1.06	7.90	90.82	1.3	6
Co/WC(A)	0.82	7.68	88.89	1.3	6
WC(B)	-	3.89	88.56	0.7	5
Ru/WC(B)	1.04	3.29	87.87	0.6	4
Co/WC(B)	0.77	3.10	86.98	0.6	4

Table 2

XPS results for the catalysts before and after reduction in H_2

(*) results obtained by deconvolution

Compound	Element	B.E. (eV) before reduction	B.E. (eV) after reduction at 673 K	B.E. (eV) after reduction at 773 K
WC(A)	W $4f_{5/2}$	33.7	-	-
	W $4f_{7/2}$	31.7	-	-
	C 1s	282.8-284.5	-	-
WC(B)	W $4f_{5/2}$	33.7	-	-
	W $4f_{7/2}$	31.7	-	-
	C 1s	282.8-284.5	-	-
Ru/WC(A)	W $4f_{5/2}$	33.9	33.8	-
	W $4f_{7/2}$	31.7	31.7	-
	Ru $3d_{3/2}$	285.8(*)	284.6(*)	-
	Ru $3d_{5/2}$	281.9(*)	280.2(*)	-
	C 1s	284.4-282.9(*)	284.4-282.9(*)	-
Ru/WC(B)	W $4f_{5/2}$	33.7-37.2	33.7	-
	W $4f_{7/2}$	35.1-31.6	31.7	-
	Ru $3d_{3/2}$	285.9(*)	284.1(*)	-
	Ru $3d_{5/2}$	281.7(*)	279.8(*)	-
	C 1s	284.2-282.6(*)	282.7(*)	-
Co/WC(A)	W $4f_{5/2}$	33.9	33.8	33.7
	W $4f_{7/2}$	31.7	31.6	31.7
	Co $2p_{1/2}$	796.4	793.4	793.2
	Co $2p_{3/2}$	780.9	778.4	778.4
	C 1s	284.4-282.8	284.4-282.8	284.4-282.7
Co/WC(B)	W $4f_{5/2}$	37.2-33.7	33.7	
	W $4f_{7/2}$	35.2-31.6	31.6	
	Co $2p_{1/2}$	797.2	793.2	
	Co $2p_{3/2}$	781.2	778.4	
	C 1s	284.6-282.7	282.7	

Table 3

Surface composition of catalysts before and after reduction in H_2 from XPS experiments and deconvolution of the C 1s and W 4f level spectrums.

catalyst	Composition $M_xWC_yO_z$	W_C/W_T	W_{Ox}/W_T	C_C/C_T	C_f/C_T	C_{Ox}/C_T	Ru/W_T	Co/W_T
WC(A)	$WC_{4.6}O_{0.9}$	0.90	0.10	0.23	0.64	0.14	-	-
WC(B)	$WC_{1.6}O_{0.8}$	0.74	0.26	0.51	0.44	0.05	-	-
Ru/WC(A)	$Ru_{0.13}WC_{4.8}O_{1.0}$	0.87	0.13	0.27	0.60	0.13	0.13	-
Ru/WC(A) (1)	$Ru_{0.12}WC_{3.6}O_{0.4}$	0.77	0.23	0.26	0.74	~ 0	0.12	-
Ru/WC(B)	$Ru_{0.49}WC_{5.7}O_{3.1}$	0.46	0.54	0.31	0.40	0.29	0.49	-
Ru/WC(B) (1)	$Ru_{0.27}WC_{0.6}O_{0.7}$	0.86	0.14	1	0	~ 0	0.26	-
Co/WC(A)	$Co_{0.15}WC_{4.1}O_{0.8}$	0.90	0.10	0.20	0.67	0.13	-	0.15
Co/WC(A) (1)	$Co_{0.10}WC_{4.2}O_{0.5}$	0.91	0.09	0.24	0.76	~ 0	-	0.10
Co/WC(A) (2)	$Co_{0.05}WC_{3.4}O_{0.3}$	0.85	0.15	0.23	0.77	~ 0	-	0.08
Co/WC(B)	$Co_{0.61}WC_{3.4}O_{3.2}$	0.46	0.54	0.15	0.62	0.23	-	0.96
Co/WC(B) (1)	$Co_{0.32}WC_{0.6}O_{0.9}$	0.77	0.23	0.72	0.28	~ 0	-	0.36

(1) reduction at 673 K, (2) reduction at 773 K,

M = Co or Ru,

W_C = tungsten carbide, W_{Ox} = tungsten oxide, W_T = total tungsten content,

C_C = carbon carbide, C_f = carbon free, C_{Ox} = carbon oxide, C_T = total carbon content

25

Table 4

Atomic ratio $(H/M)_{exp}$ calculated from hydrogen consumption of H_2-TPR profiles (M = Co or Ru). Comparison with theoretical ratio $(H/M)_{th.,}$ calculated from hydrogen required to have total reduction of the metal.

Catalyst	Ru or Co (mol)	$(H/M)_{th}$	H (mol) consumed	$(H/M)_{exp.}$	T (K)	H (mol) consumed	$(H/M)_{exp}$
			H₂-TPR peaks between 300-1200 K		Decomposition of H₂-TPR profile		
WC(B)	-	-	$5.76\ 10^{-5}$	-	-	-	-
Ru/WC(B)	$2.05\ 10^{-5}$	3	$2.14\ 10^{-4}$	10.4	300-480	$7.70\ 10^{-5}$	3.7
					480-1200	$1.37\ 10^{-4}$	6.7
Co/WC(B)	$7.14\ 10^{-5}$	2	$7.72\ 10^{-4}$	10.8	400-575	$6.00\ 10^{-5}$	0.8
					575-750	$1.80\ 10^{-4}$	2.5
					750-1000	$5.32\ 10^{-4}$	7.5

Table 5

Catalytic behavior of WC(A) catalyst ($m_{cata.}$ = 2.530 g, VSV = 6000 h^{-1})

T (K)	P (bar)	X (%)	Rate (10^{-3} mol.h^{-1}.g^{-1})	S(CO_2) (%)	S(C_1) (%)	S(C_2-C_4) (%)	S(C_{5+}) (%)	S(COH) (%)
473	20	~ 1	~ 0.3	0	26.2	36.8	15.3	21.7
493	20	~ 1	~ 0.3	0	28.9	39.8	9.3	22
533	20	5	1.6	25	39.5	49.6	5.1	5.8
473	50	2	0.6	0	25.2	30.8	6.6	37.4
493	50	3	0.9	0	30.1	38.9	8	23
533	50	16	5.1	17	45.1	46.5	4.6	3.8

Table 6

Catalytic behavior of WC supported Co and Ru catalysts, compared with parent tungsten

carbide (T = 473 K, VSV = 6000 h^{-1})

Catalyst	m cata. (g)	P (bar)	X (%)	Rate (10^{-3} mol.h^{-1}.g^{-1})	S(CO$_2$) (%)	S(C$_1$) (%)	S(C$_2$-C$_4$) (%)	S(C$_{5+}$) (%)	S(COH) (%)
WC(A)	2.530	20	~1	~0.3	0	26.2	36.8	15.3	21.7
WC(A)	2.530	50	2	0.6	0	25.2	30.8	6.6	37.4
Ru/WC(A)	2.700	20	15	4.4	0	8.4	4.6	87.0	0
Ru/WC(A)	2.700	50	23	6.8	0	20.8	9.2	70.0	0
Co/WC(A)	2.672	20	~1	~0.3	0	21.2	27.0	46.0	5.8
Co/WC(A)	2.672	50	4	1.2	0	8.8	13.3	64.1	13.8
WC(B)	2.480	20	~1	~0.3	0	40.1	37.9	22.0	0
Ru/WC(B)	2.406	20	~1	~0.3	0	34.2	37.4	28.4	0
Co/WC(B)	2.474	20	7	2.3	0	28.0	31.4	40.6	0

28
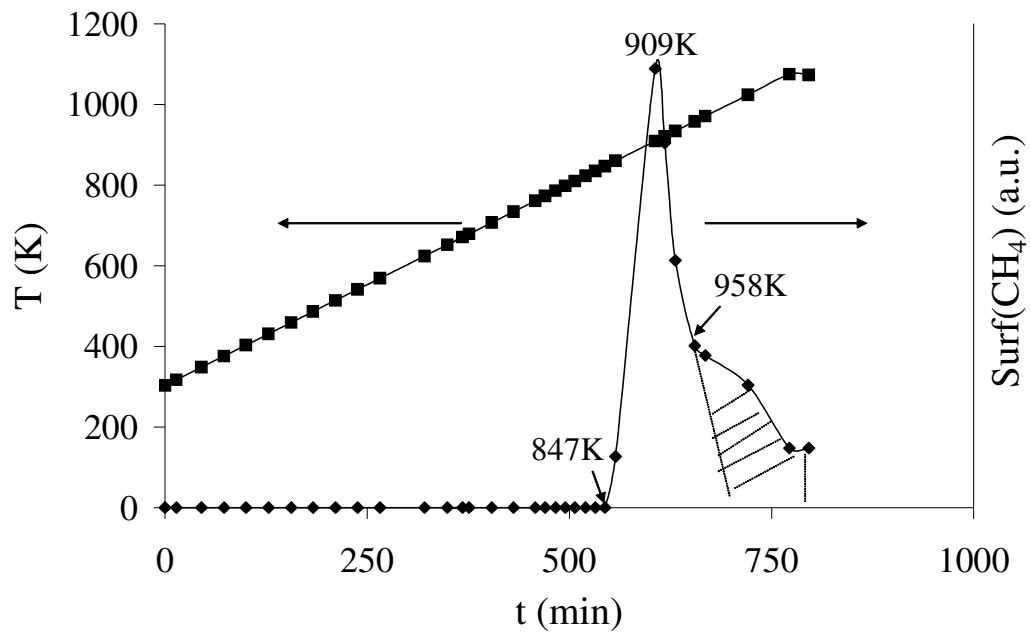
Fig. 1. Variation of the area of CH_4 during the cleaning procedure of WC(B).

Hachures correspond to surface decarburization.
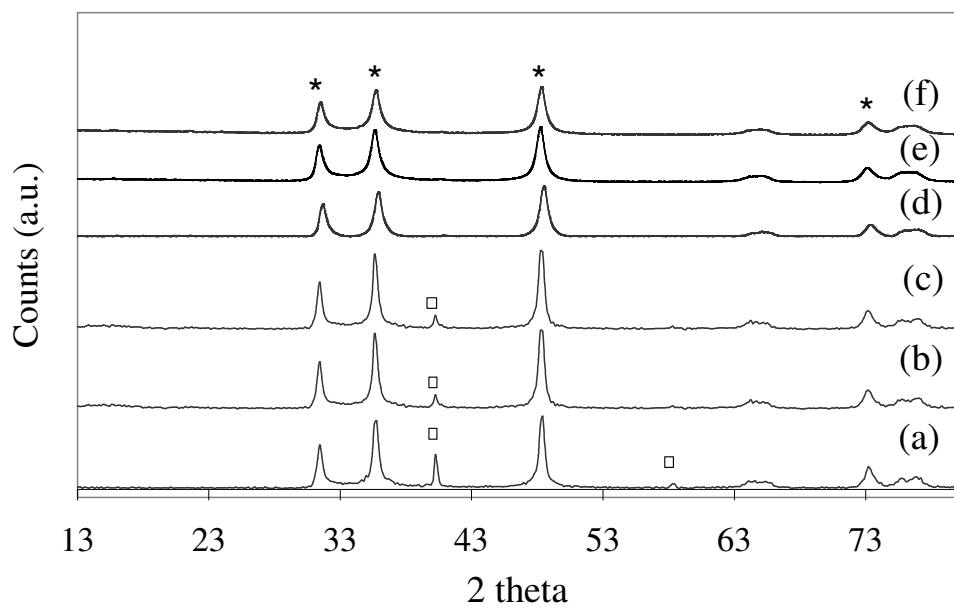
Fig. 2. XRD pattern of: (a) WC(B), (b) Co/WC(B), (c) Ru/WC(B), (d) WC(A),

(e) Co/WC(A), (f) Ru/WC(A).

∗ : lines of WC,   : lines of W metal
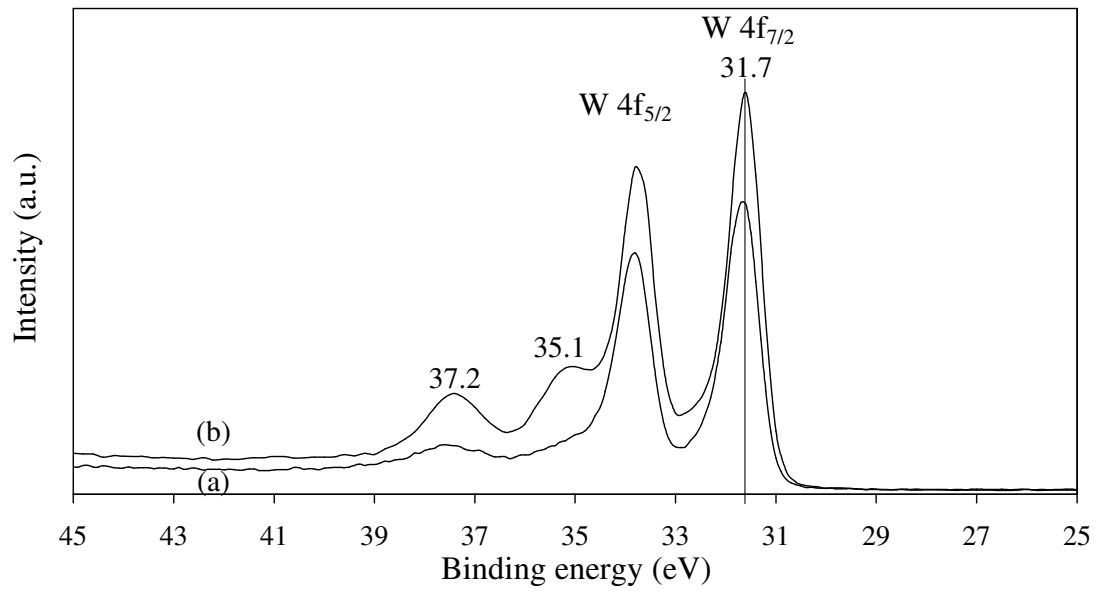
Fig. 3. W 4f XPS spectrums of: (a) WC(A), (b) WC(B).
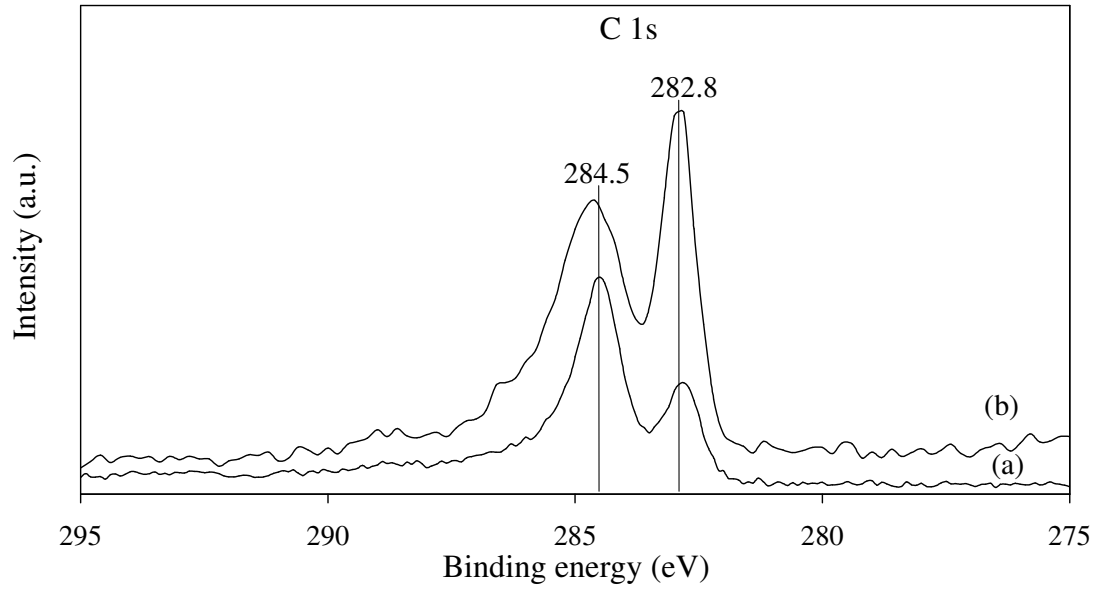
Fig. 4. C 1s XPS spectrums of: (a) WC(A), (b) WC(B).
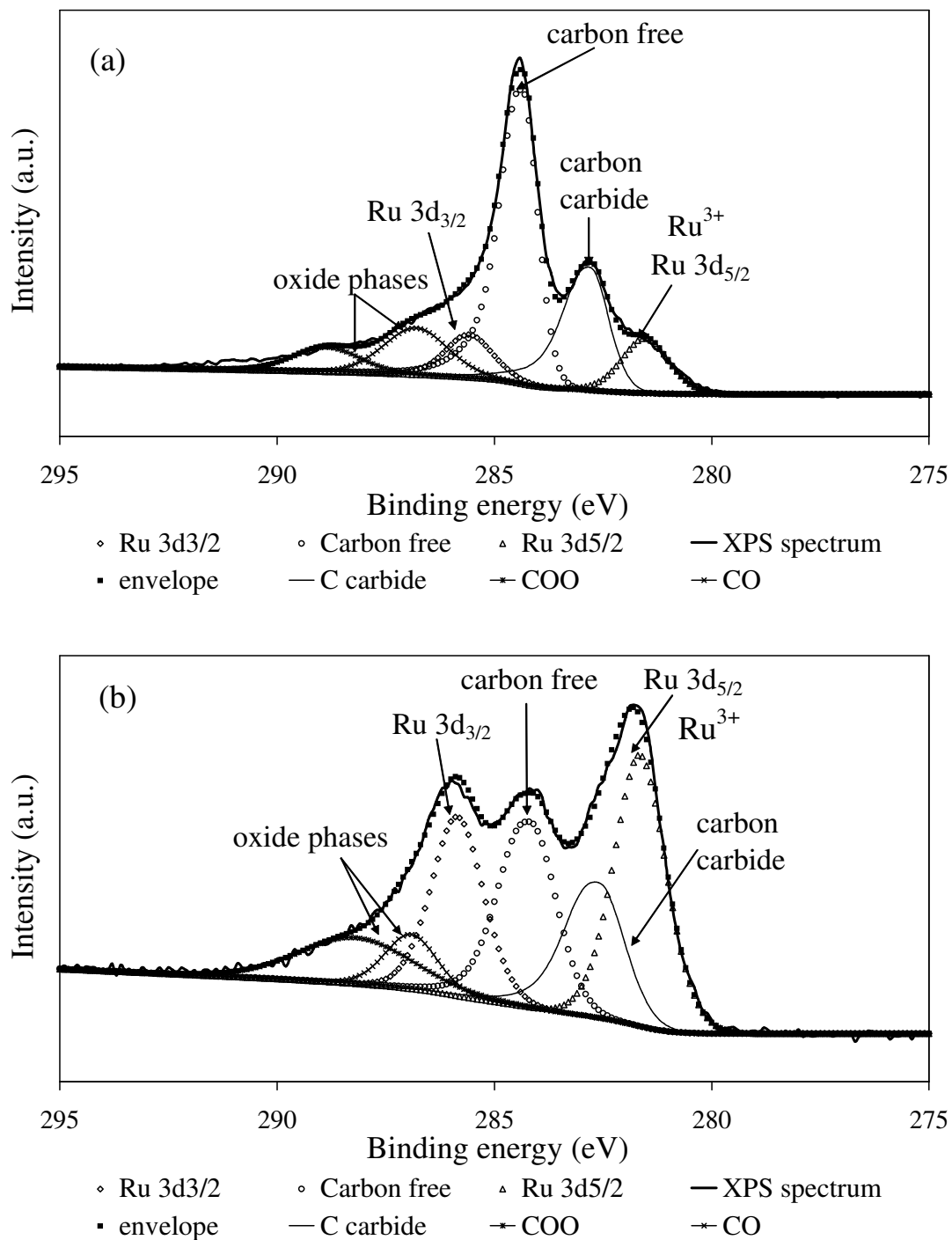
Fig. 5. Deconvolution of C 1s and Ru 3d XPS spectrums of: (a) Ru/WC(A), (b) Ru/WC(B).

33
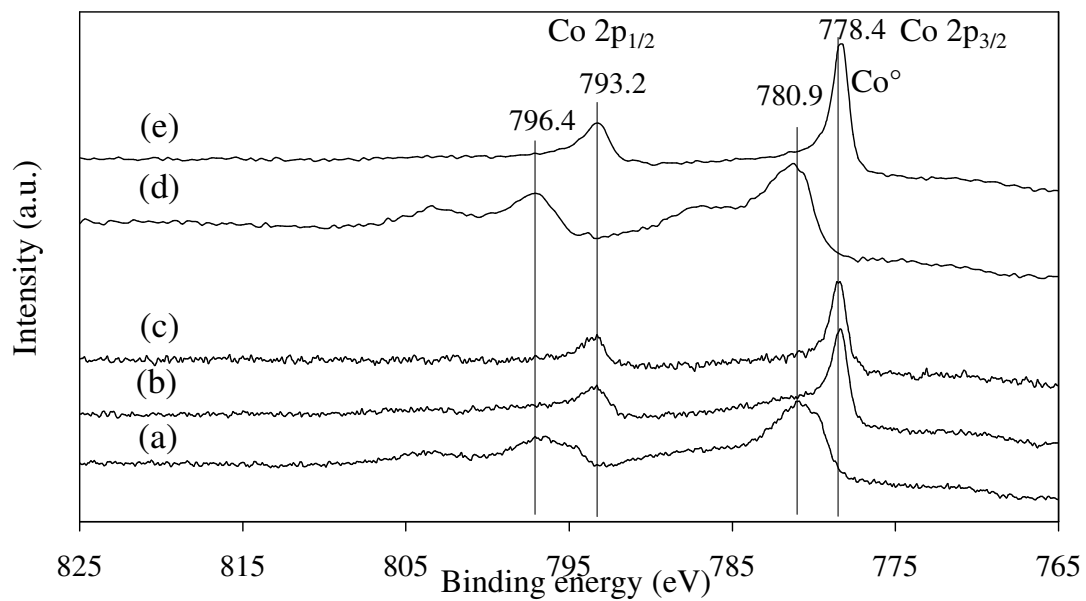
Fig. 6. Co 2p XPS spectrums of: Co/WC(A) (a) before reduction in H_2, (b) after reduction in H_2 at 673 K, (c) after reduction in H_2 at 773 K, Co/WC(B) (d) before reduction in H_2, (e) after reduction in H_2 at 673 K.
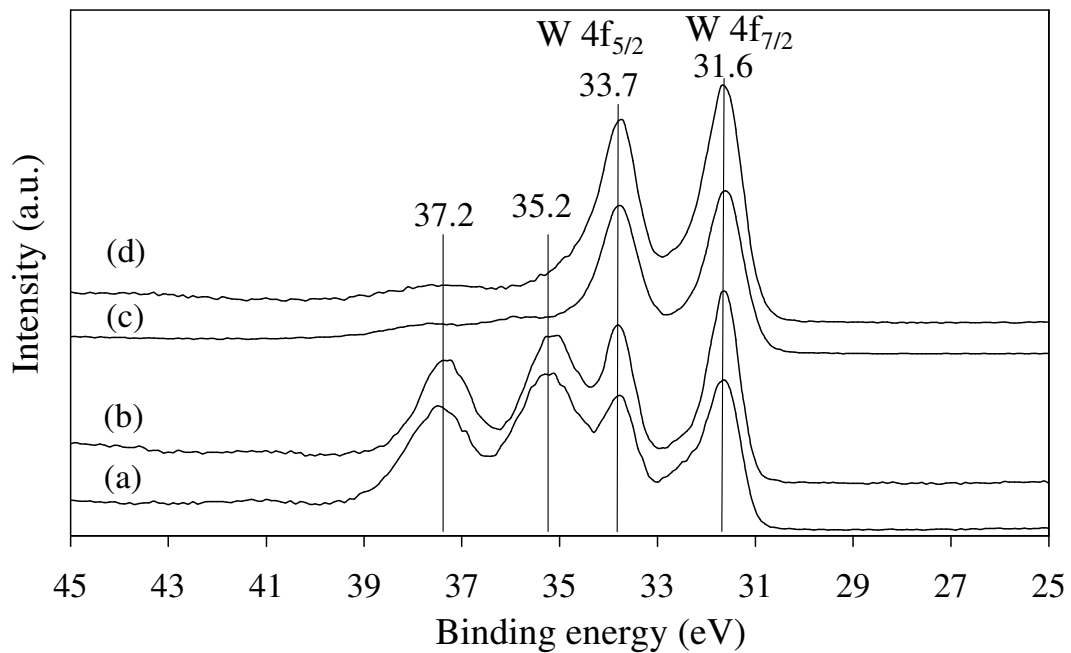
Fig. 7. W 4f XPS spectrums of: (a) Co/WC(B) before reduction in H_2, (b) Ru/WC(B) before reduction in H_2, (c) Co/WC(B) after reduction in H_2 at 673 K, (d) Ru/WC(B) after reduction in H_2 at 673 K.
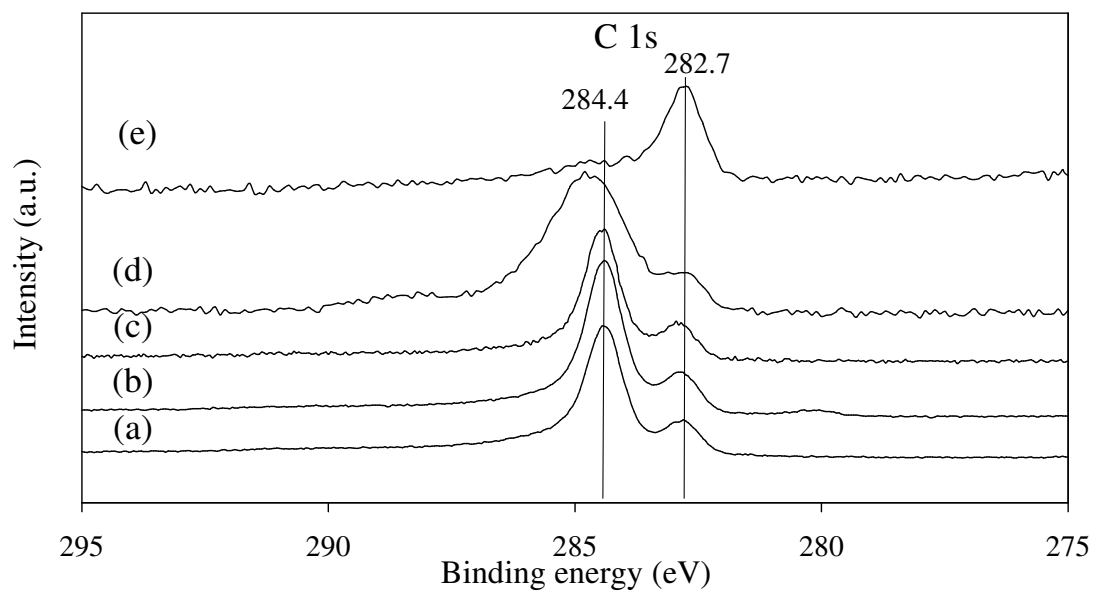
Fig. 8. C 1s XPS spectrums of: Co/WC(A) (a) before reduction in H_2, (b) after reduction at 673 K in H_2, (c) after reduction at 773 K in H_2, Co/WC(B) (d) before reduction in H_2, (e) after reduction in H_2 at 673 K.
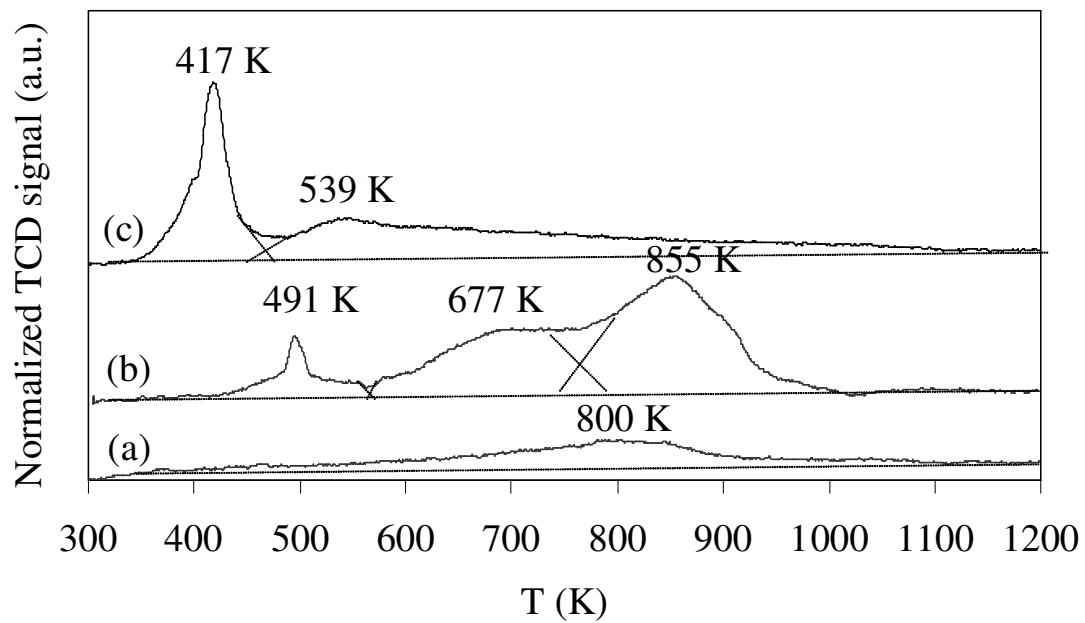
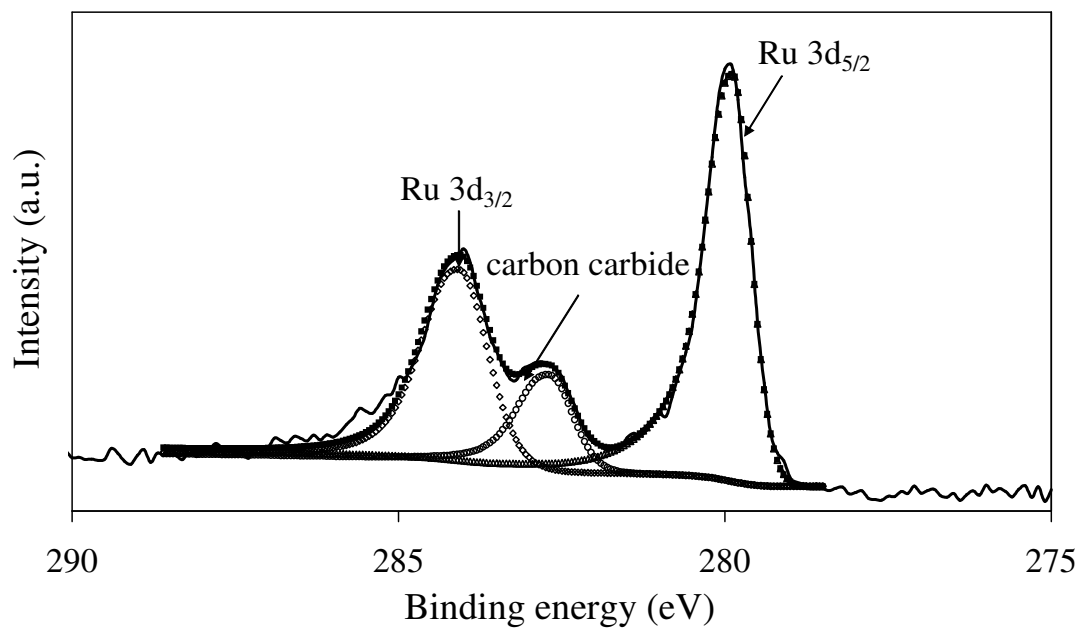Fig. 9. H$_2$-TPR profiles (5 K.min^{-1}) of: (a) WC(B), (b) Co/WC(B), (c) Ru/WC(B)

37
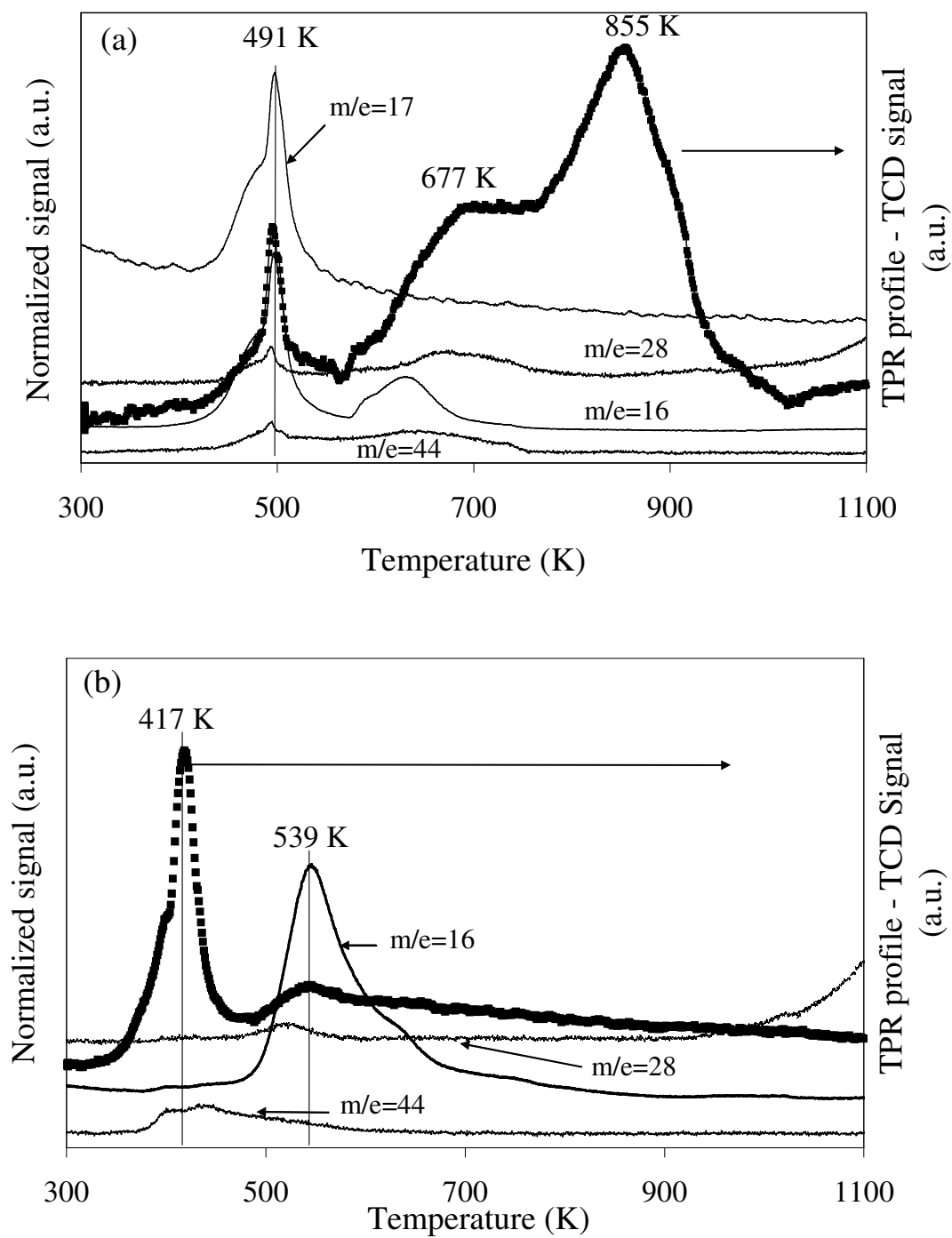
Fig. 10. H$_2$-TPR profile followed by mass spectroscopy for: (a) Co/WC(B), (b) Ru/WC(B).
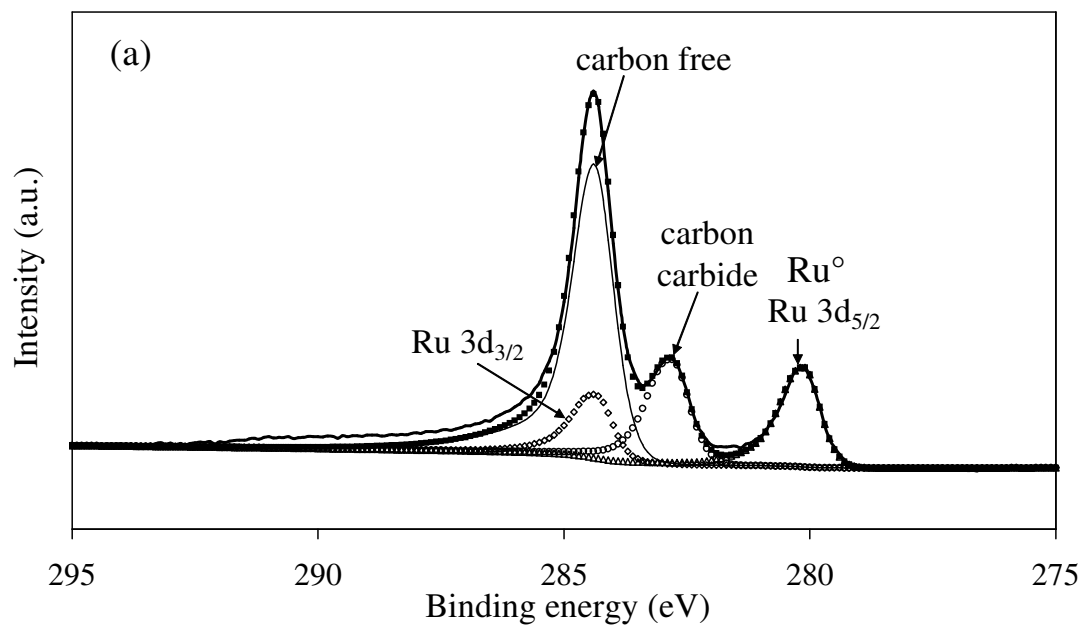
Fig. 11. Deconvolution of C 1s and Ru 3d XPS spectrums of catalysts after reduction in hydrogen at 673 K: (a) Ru/WC(A), (b) Ru/WC(B).
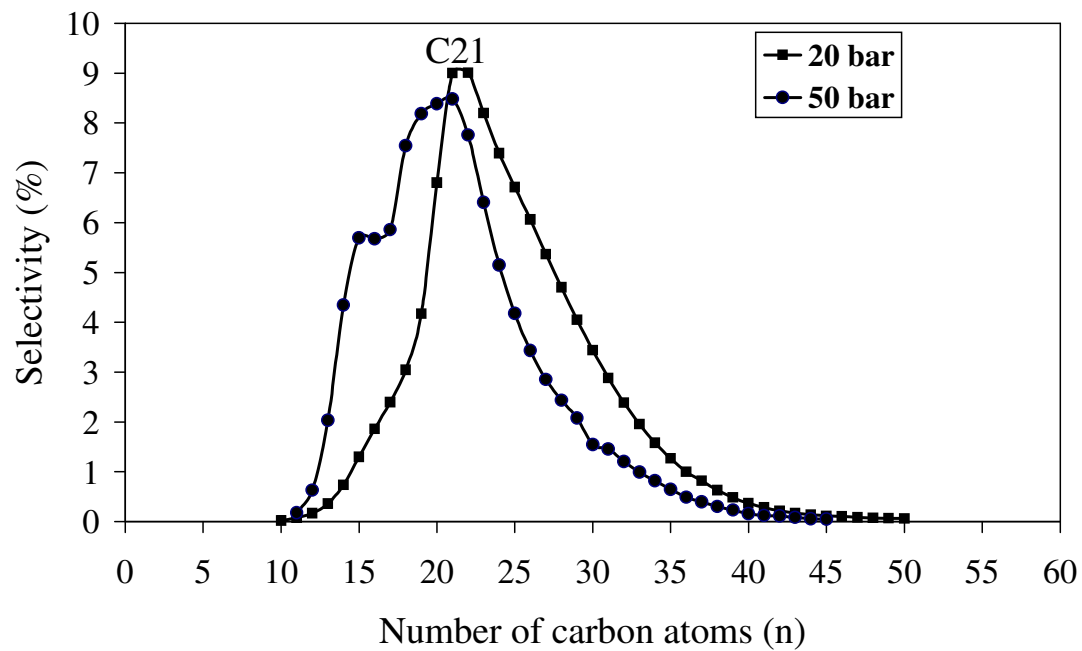
Fig. 12. Repartition of hydrocarbons products obtained in the hot condenser for Ru/WC(A) at 473 K.